JOC Article

Enantioselective [6π]-Photocyclization Reaction of an Acrylanilide Mediated by a Chiral Host. Interplay between Enantioselective Ring Closure and Enantioselective Protonation

Thorsten Bach,*,† Benjamin Grosch,† Thomas Strassner,‡,§ and Eberhardt Herdtweck‡,||

Lehrstuhl für Organische Chemie I, Technische Universität München, D-85747 Garching, Germany, and Lehrstuhl für Anorganische Chemie, Technische Universität München, D-85747 Garching, Germany

thorsten.bach@ch.tum.de

Received October 24, 2002

The [6π]-photocyclization of the anilides **1a** and **5** was studied in the absence and in the presence of the enantiomerically pure chiral lactam **4**. The relative configuration of the products was unambiguously established by single-crystal X-ray crystallography and by NMR spectroscopy. A significant enantiomeric excess was observed upon reaction of compound **1a** to its photocyclization products at −55 °C employing lactam **4** as a chiral complexing agent in toluene as the solvent (66% yield). The trans product *ent*-**3a** was obtained in 57% ee, and the minor diastereoisomer (trans/cis = 73/27), cis product *ent*-**2a**, was obtained in 30% ee. DFT calculations were conducted modeling the complexation of intermediates **8** and *ent*-**8** to host **4**. In agreement with steric arguments concerning the conrotatory ring closure of **1a**, the formation of *ent*-**8** is favored leading to the more stable complex **4**·*ent*-**8** as compared to **4**·**8**. Whereas the enantioselectivity in the photocyclization to trans compound *ent*-**3a** increased upon reduction in the reaction temperature, the enantiomeric excess in the formation of cis compound *ent*-**2a** went through a maximum at −15 °C (45% ee) and decreased at lower temperatures. Deuteration experiments conducted with the pentadeuterated analogue of **1a**, d^5-**1a**, revealed that the protonation of the intermediates **8** and *ent*-**8** is influenced by chiral amide **4**. In the formation of *ent*-**3a/3a**, both the enantioselective ring closure and the enantioselective protonation by amide **4** favor the observed (6a*S*,10a*S*)-configuration of the major enantiomer *ent*-**3a**. In the formation of *ent*-**2a/2a**, the enantioselective ring closure (and the subsequent diastereoselective protonation) favors the (6a*R*,10a*S*)-configuration that is found in compound **2a**. Contrary to that, the enantioselective protonation by amide **4** shows a preference for *ent*-**2a** with the (6a*S*,10a*R*)-configuration.

Introduction

Acryl- and aroylenamides of the general structure **A** undergo a photochemically allowed conrotatory [6π]-cyclization[1,2] reaction. If one of the two rings, I or II, is an arene or a hetarene, a subsequent tautomerization of intermediate **B** occurs regioselectively and yields either product **C** or product **D**.[3] Many variants of this useful transformation have been explored[4] and have been applied to the synthesis of naturally occurring heterocycles.[5,6] Under oxidative conditions, the formation of a central pyridone ring **E** is facile especially if both rings I and II are aromatic.[7]

The reaction of acrylanilides to the corresponding 3,4-dihydroquinolin-2-ones was first described by Chapman et al.[8] and extensively studied by Ninomiya and coworkers.[9] The reactions proceed cleanly and with high

† Lehrstuhl für Organische Chemie I.

‡ Lehrstuhl für Anorganische Chemie.

§ To whom inquiries about the DFT calculations should be addressed.

|| To whom inquiries about the X-ray analyses should be addressed.

(1) General reviews: (a) Laarhoven, W. H. *Org. Photochem.* **1989**, *10*, 163−308. (b) Laarhoven, W. H. *Org. Photochem.* **1987**, *9*, 129−224. (c) Mallory, F. B.; Mallory, C. W. *Org. React.* **1984**, *30*, 1−456. (d) Laarhoven, W. H. *Recl.: J. R. Neth. Chem. Soc.* **1983**, *102*, 241−254. (e) Laarhoven, W. H. *Recl.: J. R. Neth. Chem. Soc.* **1983**, *102*, 185−204. (f) Tominaga, Y.; Castle, R. N. *J. Heterocycl. Chem.* **1996**, *33*, 523−538.

(2) For a review on asymmetric photoreactions of α,β-unsaturated carboxylic acid derivatives and enones: Pete, J.-P. *Adv. Photochem.* **1996**, *21*, 135−216.

(3) Reviews: (a) Ninomiya, I.; Naito, T. *Heterocycles* **1981**, *15*, 1433−1462. (b) Lenz, G. R. *Synthesis* **1978**, 489−518. (c) Zeller, K.-P. In *Houben-Weyl Methods of Organic Chemistry*; Müller, E., Ed.; Thieme: Stuttgart, 1975; Vols. 4 and 5, pp 542−546.

(4) Examples: (a) Ninomiya, I.; Naito, T.; Mori, T. *J. Chem. Soc., Perkin Trans. 1* **1973**, 505−509. (b) Lenz, G. R. *J. Org. Chem.* **1974**, *39*, 2846−2851. (c) Kanaoka, Y.; Itoh, K.; Hatanaka, Y.; Flippen, J. L.; Karle, I. L., Witkop, B. *J. Org. Chem.* **1975**, *40*, 3001−3003. (d) Lenz, G. R. *J. Heterocycl. Chem.* **1979**, *16*, 433−437. (e) Kanaoka, Y.; San-nohe, K. *Tetrahedron Lett.* **1980**, *21*, 3893−3896. (f) Ninomiya, I.; Yamamoto, O.; Kiguchi, T.; Naito, T. *J. Chem. Soc., Perkin Trans. 1* **1980**, 203−207. (g) Ninomiya, I.; Kiguchi, T.; Naito, T. *J. Chem. Soc., Perkin Trans. 1* **1983**, 208−211. (h) Bates, R. B.; Kane, V. V.; Martin, A. R.; Mujumdar, R. B.; Ortega, R.; Hatanaka, Y.; San-nohe, K.; Kanaoka, Y. *J. Org. Chem.* **1987**, *52*, 3178−3180. (i) Fodor, L.; Szabó, J.; Bernáth, G.; MacLean, D. B.; Smith, R. W.; Ninomiya, I.; Naito, T. *J. Heterocycl. Chem.* **1989**, *26*, 333−337. (j) Yamaguchi, S.; Yokoi, T.; Yamada, M.; Arai, H.; Uchizo, Y.; Kawase, Y. *J. Heterocycl. Chem.* **1990**, *27*, 1003−1005.

(5) Reviews: (a) Ninomiya, I.; Naito, T. In *The Alkaloids*; Brossi, A., Ed.; Academic Press: San Diego, 1983; Vol. 22, pp 189−279. (b) Ninomiya, I.; Yamamoto, O.; Kiguchi, T.; Naito, T.; Ishii, H. *Heterocycles* **1977**, *6*, 1730−1734. Ninomiya, I. *Heterocycles* **1974**, *2*, 105−123.

10.1021/jo026602d CCC: $25.00
Published on Web 01/04/2003

yields in a variety of solvents (e.g., ether, benzene, and methanol). The diastereomeric ratio depends on the solvent. In an aprotic solvent, the tautomerization occurs to a large extent via a thermally allowed suprafacial hydrogen 1,5-shift and yields preferentially the trans product. In protic solvents or in the presence of Brønsted acids, the proton is delivered intermolecularly to intermediates of type **B** and the cis isomer prevails. Enantioselective solid-state [6π]-photocyclization reactions have been studied by Toda et al.[10] Inclusion crystals[11] of acrylanilides with tartaric acid-derived 1,4-dioxaspiro-[4.4]nonanes and -[4.5]decanes yielded predominantly the trans products in high enantiomeric excess (41−70% yield, up to 98% ee). In a detailed study it was demonstrated that the enantiomeric excess is a result of the chiral conformation in the crystalline clathrate environment provided by the chiral host. The C−C bond formation step is decisive for the absolute configuration of the product. The formation of enantiomerically enriched photocyclization products in solution was reported by Ninomiya et al.[12] They used an external chiral proton source, (+)-di(*p*-toluoyl)tartaric acid (DTTA), to achieve an enantioselective protonation of the intermediate zwitterion. The best results are summarized in Scheme 2. The photocyclization reaction of anilides **1** to tetrahydrophenathridinones **2** and **3** was conducted at 5−10 °C in a solvent mixture. The protonation step and not the C−C bond formation step is selectivity determining. The ee value is low for the major cis isomer **2** and only slightly higher for the minor trans isomer **3**. The intermolecular protonation by the chiral acid occurs at carbon atom C-6a and is responsible for the enantiomeric excess. An explanation for the face discrimination has been proposed.[12]

We became interested in the [6π]-photocyclization in connection with our work[13] on enantioselective photochemical reactions[14] in solution. Host compounds such as lactam **4**[15] (Figure 1) have been established as versatile complexing agents for achieving moderate to high enantioselectivities in photocycloaddition,[16] Norrish−Yang cyclization,[17] and [4π]-photocyclization reactions[16c] of lactams. The hosts interact with lactams by two-point hydrogen binding, which facilitates the

SCHEME 1

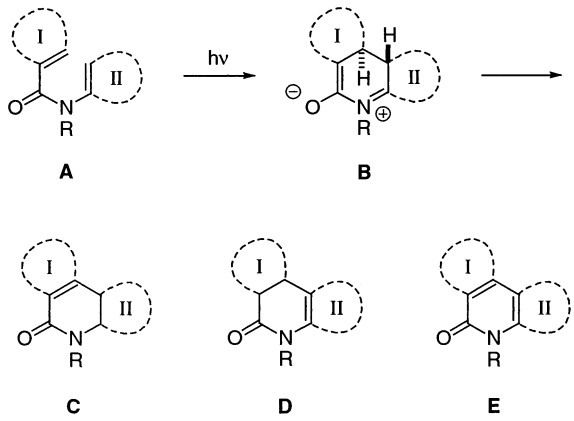

SCHEME 2

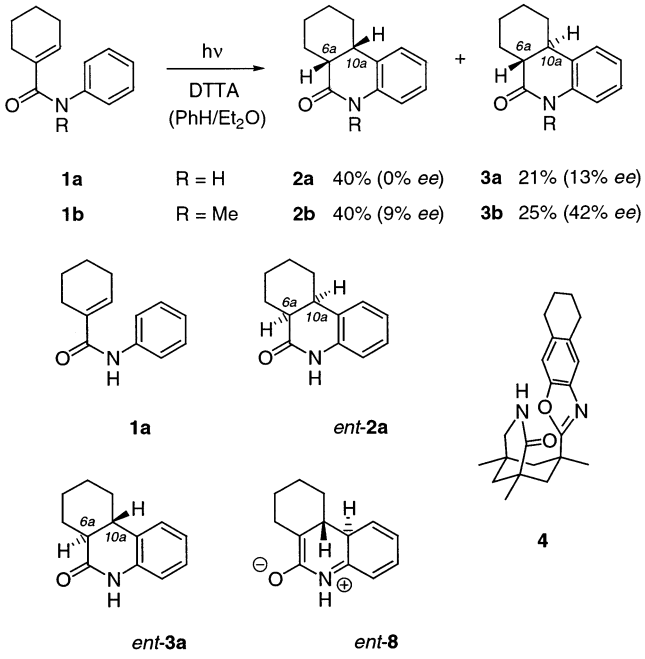

(6) For recent applications, see: (a) Rigby, J. H.; Maharoof, U. S. M.; Mateo, M. E. *J. Am. Chem. Soc.* **2000**, *122*, 6624−6628. (b) Bois, F.; Gardette, D.; Gramain, J.-C. *Tetrahedron Lett.* **2000**, *41*, 8769−8772. (c) Schultz, A. G.; Holoboski, M. A.; Smyth, M. S. *J. Am. Chem. Soc.* **1996**, *118*, 6210−6219. (d) Naito, T.; Yuumoto, Y.; Kiguchi, T.; Ninomiya, I. *J. Chem. Soc., Perkin Trans. 1* **1996**, 281−288. (e) Heathcock, C. H.; Norman, M. H.; Dickman, D. A. *J. Org. Chem.* **1990**, *55*, 798−811.

(7) (a) Kanaoka, Y.; Itoh, K. *Synthesis* **1972**, 36. (b) Winterfeldt, E.; Altmann, H. J. *Angew. Chem., Int. Ed. Engl.* **1968**, *7*, 466. (c) Kanaoka, Y.; San-nohe, K.; Hatanaka, Y.; Itoh, K.; Machida, M.; Terashima, M. *Heterocycles* **1977**, *6*, 29−32. (d) Yamaguchi, S.; Oh-hira, Y.; Yamada, M.; Michitani, H.; Kawase, Y. *Bull. Chem. Soc. Jpn.* **1990**, *63*, 952−954.

(8) (a) Cleveland, P. G.; Chapman, O. L. *Chem. Commun.* **1967**, 1064−1065. (b) Chapman, O. K.; Adams, W. R. *J. Am. Chem. Soc.* **1968**, *90*, 2333−2342. (c) See also: Ogata, Y.; Takai, K.; Ishino, I. *J. Org. Chem.* **1971**, *36*, 3975−3979.

(9) (a) Ninomiya, I.; Yamauchi, S.; Kiguschi, T.; Shinobara, A.; Naito, T. *J. Chem. Soc., Perkin Trans. 1* **1974**, 1747−1751. (b) Ninomiya, I.; Kiguchi, T.; Yamauchi, S.; Naito, T. *J. Chem. Soc., Perkin Trans. 1* **1976**, 1861−1865. (c) Ninomiya, I.; Kiguchi, T.; Naito, T. *Heterocycles* **1978**, *9*, 1023−1029. (d) Ninomiya, I.; Kiguchi, T.; Yamauchi, S.; Naito, T. *J. Chem. Soc., Perkin Trans. 1* **1980**, 197−202. (e) Ninomiya, I.; Hashimoto, C.; Kiguchi, T.; Naito, T. *J. Chem. Soc., Perkin Trans. 1* **1983**, 2967−2971.

(10) (a) Tanaka, K.; Kakinoki, O.; Toda, F. *Chem. Commun.* **1992**, 1053−1054. (b) Toda, F.; Miyamoto, H.; Kanemoto, K.; Tanaka, K.; Takahashi, Y.; Takenaka, Y. *J. Org. Chem.* **1999**, *64*, 2096−2102. (c) Ohba, S.; Hosomi, H.; Tanaka, K.; Miyamoto, H.; Toda, F. *Bull. Chem. Soc. Jpn.* **2000**, *73*, 2075−2085.

(11) Reviews: (a) Toda, F. *Acc. Chem. Res.* **1995**, *28*, 480−486. (b) Tanaka, K.; Toda F. *Chem. Rev.* **2000**, *100*, 1025−1074.

(12) Naito, T.; Tada, Y.; Ninomiya, I. *Heterocycles* **1984**, *22*, 237−240.

(13) Initial studies: (a) Bach, T.; Bergmann, H.; Harms, K. *J. Am. Chem. Soc.* **1999**, *121*, 10650−10651. (b) Bach, T. *Synlett* **2000**, 1699−1707. (c) Bach, T.; Bergmann, H.; Brummerhop, H.; Lewis, W.; Harms, K. *Chem. Eur. J.* **2001**, *7*, 4512−4521.

(14) Reviews: (a) Everitt, S. R. L.; Inoue, Y. In *Molecular and Supramolecular Photochemistry: Organic Molecular Photochemistry*; Ramamurthy, V., Schanze, K. S., Eds.; Dekker: New York, 1999; Vol. 3, pp 71−130. (b) Inoue, Y. *Chem. Rev.* **1992**, *92*, 741−770. (c) Rau, H. *Chem. Rev.* **1983**, *83*, 535−547.

(15) Bach, T.; Bergmann, H.; Grosch, B.; Harms, K.; Herdtweck, E. *Synthesis* **2001**, 1395−1405.

(16) (a) Bach, T.; Bergmann, H.; Harms, K. *Angew. Chem., Int. Ed.* **2000**, *39*, 2302−2304. (b) Bach, T.; Bergmann, H. *J. Am. Chem. Soc.* **2000**, *122*, 11525−11526. (c) Bach, T.; Bergmann, H.; Harms, K. *Org. Lett.* **2001**, *3*, 601−603. (d) Bach, T.; Bergmann, H.; Grosch, B.; Harms, K. *J. Am. Chem. Soc.* **2002**, *124*, 7982−7990.

(17) (a) Bach, T.; Aechtner, T.; Neumüller, B. *Chem. Commun.* **2001**, 607−608. (b) Bach, T.; Aechtner, T.; Neumüller, B. *Chem. Eur. J.* **2002**, *8*, 2464−2475.

TABLE 1. Preparation of Racemic Compounds *rac*-2a, *rac*-3a, *rac*-6, and *rac*-7 by Photocylization under Various Conditions

entry	substrate	*c* (mM)	solvent	temp (°C)	*rac*-product	trans/cis[a]	yield (%)[b]
1	**1a**	4	toluene	35	**3a**/**2a**	36/64	77
2	**1a**	4	toluene	−15	**3a**/**2a**	36/62	66
3	**1a**	4	toluene	−55	**3a**/**2a**	46/54	65
4	**1a**	4	Et_2O	35	**3a**/**2a**	46/54	82
5	**5**	10	toluene	35	**7**/**6**	54/46	61
6	**5**	10	toluene	−15	**7**/**6**	—[c]	66

[a] Diastereomeric ratio was determined by GC analysis of the crude product mixture. [b] Yield of isolated product (mixture of the two diastereoisomers). [c] Not determined.

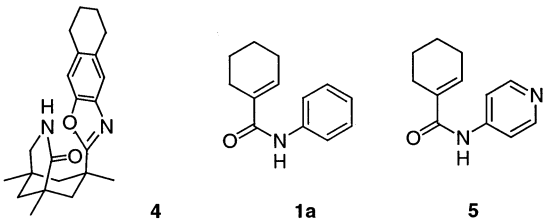

FIGURE 1. Structure of host **4** employed in the enantioselective [6π]-photocyclization of compounds **1a** and **5**.

positioning of the substrates in a chiral environment. Acyclic amides had not yet been tested in this context, and we wondered whether these substrates would be amenable to an enantioselective reaction in the presence of host **4**. We selected the previously used anilide **1a** as the substrate, which exhibits a hydrogen bond acceptor (NH) and a hydrogen bond donor (C═O) site. Since a cisoid arrangement of the amide is required for a successful photocyclization, we were optimistic that binding to host **4** and a face differentiation could be achieved. For comparison, the analogous pyridine **5** was also studied. It was suspected, however, that the basic pyridine nitrogen atom would interfere with the hydrogen bonding and that its reaction would consequently be less selective.

In this account, we report on the results of the study that focused mainly on the [6π]-cyclization of substrate **1a**. Contrary to our expectations, it turned out that the enantioselectivity depends not only on the binding to the host and the enantioface differentiation but also on the ability of the host to act as a Brønsted acid. The study was accompanied by deuteration experiments, which shed light on the mechanism of the reaction, and by DFT calculations, which give a more detailed picture of the binding to hosts of type **4**.

Results and Discussion

Photocyclization and Assessment of the Product Configuration. To obtain racemic compounds for comparison, amides **1a** and **5** were irradiated in an immersion apparatus with a mercury high-pressure lamp (Original Hanau TQ 150). A Vycor filter (90% transmission at 330 nm, 45% transmission at 250 nm) was used to cut off short-wavelength UV light. Phenyl derivative **1a** yielded the racemic cis and trans products *rac*-**2a** and *rac*-**3a**, respectively (Table 1). Pyridyl derivative **5** gave the corresponding cis and trans products *rac*-**6** and *rac*-**7**, respectively (Figure 2). Whereas cis product *rac*-**2a** was favored in the former case (entries 1−4), a slight preference for trans isomer *rac*-**7** (entry 5) was observed in the latter case.

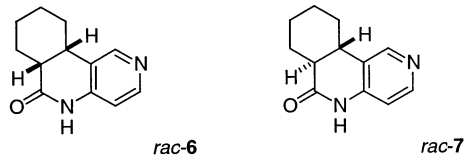

FIGURE 2. Structure of photocyclization products *rac*-**6** and *rac*-**7**.

In ether as the solvent, the simple diastereoselectivity decreased (entry 4 in Table 1). Surprisingly, a decrease in the simple diastereoselectivity was also observed while decreasing the reaction temperature (entries 1−3). This issue will be discussed in more detail later.

It turned out that compounds *rac*-**2a** and *rac*-**3a** are separable by HPLC (reverse-phase column YMC ODS-A; eluent, 30/70 → 60/40 MeCN/H_2O). Moreover, all stereoisomers (enantiomers and diastereoisomers) could be separated by chiral GC (Suppelco β-Dex 325, 160 → 200 °C at 0.5 K/min), which in turn facilitated the determination of ee values. The assignment of the relative configuration was based on reported data[9a] and supported by the NMR data of the individual compounds. The coupling constant ($^3J_{HH}$) of the two protons at C-6a and C-10a is 4.8 Hz for the cis isomer *rac*-**2a** and 14.1 Hz for trans isomer *rac*-**3a**. In addition, we obtained crystals of both diastereoisomers that were suitable for single-crystal X-ray crystallography. The molecular structures of the starting material **1a**, of the minor diastereoisomer *rac*-**2a**, and of the major trans diastereoisomer *rac*-**3a** are found in the Supporting Information.

In a second set of experiments, the irradiation of substrates **1a** and **5** was conducted in the presence of host **4**. The experimental setup was identical to the setup used in the racemic case. Upon determination of the simple diastereoselectivity, the host was removed by column chromatography and the purified mixture of diastereoisomers was studied by chiral GC. The choice of Vycor glass as the filter was a consequence of the strong decrease in host recovery upon using quartz glass (90% transmission at 250 nm). With duran glass (5% transmission at 250 nm), the reaction remained incomplete. The recovery yields are also provided in Table 2. In all cases in which host **4** and substrate **1a** were used (entries 1−9), the major enantiomer detected was *ent*-**3a** for the isolated trans diastereoisomer and *ent*-**2a** for the isolated cis diastereoisomer (vide infra). The determination of the absolute configuration was not possible for the products derived from substrate **5** (entries 10 and 11). Compared to the earlier results obtained in the absence of host **4** (Table 1), the trans/cis ratio shifted in

TABLE 2. Preparation of Enantiomerically Enriched Compounds *ent*-2a, *ent*-3a, 6/*ent*-6, and 7/*ent*-7 by Photocyclization in the Presence of Host 4

entry	substrate	c_{amide} (mM)	solvent	c_{host} (mM)	temp (°C)	time (min)[a]	rec. host (%)[b]	yield (%)[c]	trans/cis[d]	ee_{trans} (%)[e]	ee_{cis} (%)[e]
1	**1a**	4	toluene	4.8	35	120	86	75	52/48	35	34
2	**1a**	30	toluene	36	35	120	–[f]	–[f]	52/48	35	39
3	**1a**	4	toluene	9.6	35	120	86	75	51/49	38	37
4	**1a**	4	toluene	4.8	−15	135	75	63	55/45	39	36
5	**1a**	4	toluene	9.6	−15	135	78	70	58/42	45	45
6	**1a**	4	toluene	4.8	−55	180	76	60	71/29	49	28
7	**1a**	4	toluene	9.6	−55	180	74	66	73/27	57	30
8	**1a**	4	Et_2O	4.8	35	180	84	82	58/42	22	28
9	**1a**	4	Et_2O	9.6	35	180	84	82	58/42	28	34
10	**5**	6	toluene	14.4	35	90	77	79	57/43	25	10
11	**5**	2.5	toluene	6	−15	135	79	90	55/45	8	13

[a] Time after which the conversion was complete. [b] Yield of recovered host after the enantioselective photochemical reaction. [c] Yield of isolated product (mixture of the two diastereoisomers). [d] The diastereomeric ratio was determined by GC analysis of the crude product mixture. [e] The enantiomeric excess was determined by chiral GC analysis. [f] Not determined.

favor of the trans diastereoisomer. In addition, the trans preference increased significantly at lower temperatures (entries 6 and 7).

Irradiation experiments conducted at room temperature in toluene revealed significant enantioselectivities (entries 1−3) for both the trans and cis products. Neither the absolute substrate concentration nor the relative concentration of substrate/host altered the enantioselectivity. In all earlier experiments,[16,17] an increased host concentration (relative to the substrate) had led to a significant increase in the product ee. It was even more surprising that the major enantiomers *ent*-**3a** and *ent*-**2a** had identical absolute configurations at the stereogenic carbon atom C-6a but differed in the absolute configuration at the stereogenic carbon atom C-10a, which is formed in the C−C bond-forming step. In the more polar solvent diethyl ether (entries 8 and 9), the enantioselectivity was lower, which was in line with our expectations. Pyridine derivative **5** gave the corresponding products **6**/*ent*-**6** and **7**/*ent*-**7** in very modest enantioselectivities (entry 10). The baseline separation (GC) was not complete for trans diastereoisomer **7**/*ent*-**7**, and its ee value was not accurately determined. In this respect, the ee value obtained at lower temperatures (entry 11) was not fully accurate either. As both values remained low, substrate **5** was not studied more closely. Lowering the reaction temperature in the irradiation of compound **1a** had an astonishing effect (entries 4−7). Whereas the enantiomeric excess in which enantiomer *ent*-**3a** of the trans diastereoisomer was formed increased up to 57% ee, the enantiomeric excess for the minor diastereoisomer went through a maximum at −15 °C (entry 5) and decreased significantly at −55 °C (entries 6 and 7). The results were fully reproducible and raised the question as to which factors had an influence on the enantioselectivity.

Before this question is addressed, it should be mentioned how the absolute configuration of compounds **2a**, *ent*-**2a**, **3a**, and *ent*-**3a** was assigned. In previous work, Ninomiya et al. had found that enantiomerically pure compound **2a** is dextrorotatory with a reported specific rotation $[\alpha]_D = +22.9$ (*c* 0.48, $CHCl_3$) and that enantiomerically pure compound *ent*-**3a** is levorotatory with $[\alpha]_D = -158.8$ (*c* 0.16, $CHCl_3$). In addition, it was shown that in the *N*-methyl series, enantiomerically pure compound **2b** is dextrorotatory with a reported specific rotation $[\alpha]_D = +53.9$ (*c* 0.36, $CHCl_3$) and that enantiomerically pure compound *ent*-**3b** is levorotatory with $[\alpha]_D = -169.2$ (*c* 0.50, $CHCl_3$).[12] The compounds we isolated from the photocyclization of substrate **1a** were levorotatory. On the basis of measurements conducted with diastereomerically pure products (HPLC separation), we determined the specific rotation of *ent*-**3a** with 47% ee to be $[\alpha]_D^{20} = -68.7$ (*c* 0.42, $CHCl_3$) and that of *ent*-**2a** with 40% ee to be $[\alpha]_D^{20} = -19.7$ (*c* 0.23, $CHCl_3$). The magnitude of the specific rotation for **3a**/*ent*-**3a** was consequently in line with previous data, whereas the value we had determined for **2a**/*ent*-**2a** was higher than expected. To confirm the direction of the specific rotation, quantum chemical calculations were conducted.[18] The calculation did indeed confirm the assignment, i.e., that both *ent*-**2a** and *ent*-**3a** are levorotatory.

An additional line of evidence for the configuration assignment was derived from N-methylation of enantiomerically enriched products *ent*-**2a** and *ent*-**3a** (Scheme 3). N-Methylation of the levorotatory trans diastereoisomer *ent*-**3a** gave a mixture of trans product *ent*-**3b**, which was levorotatory, and cis diastereoisomer **2b**, which was dextrorotatory. The enantiomeric excess (47% ee) remained unchanged. The cis diastereoisomer can only be formed by epimerization at carbon atom C-6a. Cis diastereoisomer *ent*-**2b** obtained from enantiomerically enriched cis compound *ent*-**2a** was levorotatory. The result unambiguosly proved that the absolute configuration at carbon atom C-6a is responsible for the direction of the

(18) Quantum chemical calculations were performed with the TURBOMOLE suite of programs.[18a] Structures of **2a** and **3a** were fully optimized at the density functional (DFT) level employing the B3LYP hybrid functional[18b] and a Gaussian AO basis of valence-double-ζ quality, including polarization functions on nonhyrdogen atoms (SV(P)).[18c] Structures were used in subsequent calculations of the frequency-dependent optical rotation ($[\alpha]_D$) at the sodium D-line wavelength. These calculations were performed in the framework of time-dependent DFT[18d] as described in detail.[18e,f] In the TDDFT approach, aug-cc-pVDZ basis sets,[18g] the BP86 density functional,[18h] and the RI approximation[18f] were used. The results are +133 and +224 for **2a** and **3a**, respectively. (a) Ahlrichs, R.; Bär, M.; Häser, M.; Horn, H.; Kölmel, C. *Chem. Phys. Lett.* **1989**, *162*, 165. Current version: see http://www.turbomole.de. (b) Becke, A. D. *J. Chem. Phys.* **1993**, 98, 5648. Stephens, P. J.; Devlin, F. J.; Chabalowski, C. F.; Frisch, M. J. *J. Phys. Chem.* **1994**, *98*, 11623. (c) Schäfer, A.; Horn, H.; Ahlrichs, R. *J. Chem. Phys.* **1992**, *97*, 2571. (d) Bauernschmitt, R.; Ahlrichs, R. *Chem. Phys. Lett.* **1996**, *256*, 454. (e) Grimme, S. *Chem. Phys. Lett.* **2001**, *339*, 380. (f) Grimme, S.; Furche, F.; Ahlrichs, R. *Chem. Phys. Lett.* **2002**, *361*, 321. (g) Dunning, T. H. *J. Chem. Phys.* **1993**, *98*, 7059. Kendall, R. A.; Dunning, T. H.; Harrison, R. J. *J. Chem. Phys.* **1992**, *96*, 6796. (h) Becke, A. D. *Phys. Rev. A.* **1988**, *38*, 3098. Perdew, J. B. *Phys. Rev. B.* **1986**, *33*, 8822.

SCHEME 3

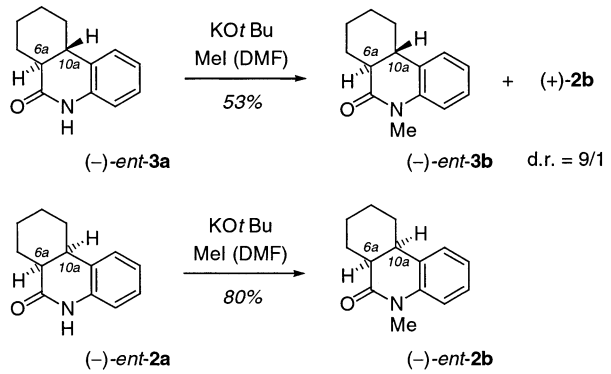

SCHEME 4

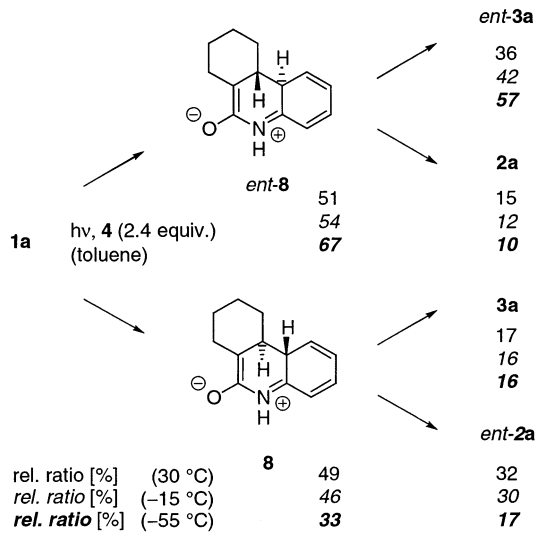

specific rotation. The major enantiomers *ent*-**3a** and *ent*-**2a** have different absolute configurations at C-10a, i.e., the stereogenic center that is formed in the ring closure step. Qualitatively, the specific rotations reported by Ninomiya et al. were confirmed.

Conrotatory Ring Closure. The degree of face differentiation in the photocyclization step can be evaluated from the data recorded in Table 2. The absolute configuration at carbon atom C-10a is established in this step and cannot be inverted in the further course of the reaction. Given zwitterionic intermediates **8** and *ent*-**8** as primary products of a conrotatory [6π]-photocyclization, it is apparent (Scheme 4) that the products *ent*-**3a** and **2a** are formed from intermediate *ent*-**8** and that the products **3a** and *ent*-**2a** are formed from intermediate **8**. Since the product distribution is known from experimental data (Table 2), the enantiomeric ratio with which *ent*-**8** is formed relative to **8** can be calculated. The data are implemented in Scheme 4 for irradiation experiments that were conducted with 2.4 equiv of host (entries 3, 5, and 7 in Table 2) in toluene as the solvent. At low temperatures (−55 °C), a significant enantioselective differentiation occurs in the presence of host **4** that leads to the preferential formation of intermediate *ent*-**8** (*ent*-**8**/**8** = 67/33).

To explain the differentiation of enantiotopic faces, we invoke a binding of amide **1a** in its cis configuration to host **4**.[19] In this arrangement, the cyclohexene moiety of

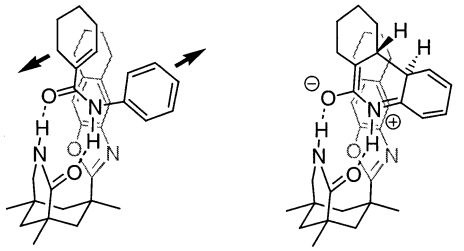

FIGURE 3. Complexation of substrate **1a** to host **4** and subsequent conrotatory photocyclization to complex **4**·*ent*-**8**.

the amide is located directly opposite the tetrahydronaphthalene moiety of the host. The phenyl group of the anilide is not in the immediate vicinity of the sterically bulky environment. Upon conrotatory ring closure, the cyclohexene ring can either turn in the direction of the tetrahydronaphthalene or it can move away and in doing so open its *Si*-face to attack from the benzene ring. According to simple molecular models, the latter movement, as schematically drawn in Figure 3, appears to be favored for steric reasons. As a consequence, the product *ent*-**8** is formed as the major product, which is still bound to the host.

By the same reasoning, product **4**·*ent*-**8** should also be thermodynamically favored over the alternative complex **4**·**8**. In the former complex, the hydrogen atom at carbon atom C-10a points away from the tetrahydronaphthalene and the cyclohexane is essentially unstrained. In the latter complex, a more strained arrangement is expected. As the diastereotopic complexes **4**·*ent*-**8** and **4**·**8** can be envisaged as the closest accessible models for the diastereotopic transition states of the photocyclization, we tried to determine their relative energy by appropriate calculations.

Density functional theory calculations (Becke3LYP/6-31G*)[20,21] were employed to study the system. The interaction energy for the complexation of **1a** by the host molecule **4** is calculated to be −10.4 kcal/mol. The bond lengths for the two NH···O bonds are 1.89 and 1.84 Å, showing that the hydrogen bonds and therefore the coordination of **1a** to **4** is weaker in this case compared to other previously studied lactam guest compounds.[16d]

(19) The equilibrium between the cis and trans rotamers of compound **1a** is in favor of the trans rotamer, which complicates any attempt to determine the complex formation quantitatively. NMR titration experiments were not conclusive. In addition, as one referee suggested, the photoexcited cis rotamer (being a stronger acid and a stronger base after photoexcitation) might be trapped in complex **4**·**1a** and consequently end up as **4**·*ent*-**8**.

(20) (a) Becke, A. D. *J. Chem. Phys.* **1993**, *98*, 5648−5652. (b) Lee, C.; Yang, W.; Parr, R. G. *Phys. Rev. B: Condens. Matter* **1988**, *37*, 785−789. (c) Vosko, S. H.; Wilk, L.; Nusair, M. *Can. J. Phys.* **1980**, *58*, 1200−1211. (d) Stephens, P. J.; Devlin, F. J.; Chabalowski, C. F.; Frisch, M. J. *J. Phys. Chem.* **1994**, *98*, 11623−11627.

(21) Frisch, M. J.; Trucks, G. W.; Schlegel, H. B.; Scuseria, G. E.; Robb, M. A.; Cheeseman, J. R.; Zakrzewski, V. G.; Montgomery, J. A., Jr.; Stratmann, R. E.; Burant, J. C.; Dapprich, S.; Millam, J. M.; Daniels, A. D.; Kudin, K. N.; Strain, M. C.; Farkas, O.; Tomasi, J.; Barone, V.; Cossi, M.; Cammi, R.; Mennucci, B.; Pomelli, C.; Adamo, C.; Clifford, S.; Ochterski, J.; Petersson, G. A.; Ayala, P. Y.; Cui, Q.; Morokuma, K.; Malick, D. K.; Rabuck, A. D.; Raghavachari, K.; Foresman, J. B.; Cioslowski, J.; Ortiz, J. V.; Stefanov, B. B.; Liu, G.; Liashenko, A.; Piskorz, P.; Komaromi, I.; Gomperts, R.; Martin, R. L.; Fox, D. J.; Keith, T.; Al-Laham, M. A.; Peng, C. Y.; Nanayakkara, A.; Gonzalez, C.; Challacombe, M.; Gill, P. M. W.; Johnson, B. G.; Chen, W.; Wong, M. W.; Andres, J. L.; Head-Gordon, M.; Replogle, E. S.; Pople, J. A. *Gaussian 98*, revision A.7; Gaussian, Inc.: Pittsburgh, PA, 1998.

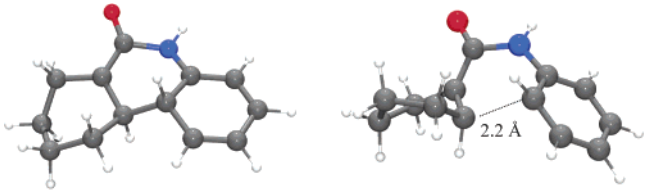

ent-**8** *ent*-$\mathbf{8_{TS}}$

FIGURE 4. Calculated structure of cyclization product *ent*-**8** and transition state *ent*-$\mathbf{8_{TS}}$ that would lead to *ent*-**8** on the S_0-hypersurface

Due to the size of the system, it has not been possible to study the diastereotopic transition states for the formation of **8** and *ent*-**8** coordinated to host **4**. In addition, the photochemical reaction proceeds via excited states and does not proceed on the S_0-hypersurface. Still, the conrotatory transition state for the formation of enantiomer *ent*-**8** from **1a** shown in Figure 4, which is calculated on the S_0-hypersurface, can be considered a model of the real transition state on the excited surface. The conformation of the calculated transistion state *ent*-$\mathbf{8_{TS}}$ provides a rough picture for the topologic change upon going from **1a** to **8**/*ent*-**8**. The forming bond in the transition state with a distance of 2.20 Å connects two carbon centers, which are right between sp^2- and sp^3-hybridization (Figure 4).

The complexation of **8** and *ent*-**8** to **4** leads to diastereomeric complexes **8·4** and *ent*-**8·4**, as shown in Figure 5. On the basis of the previous argument that these complexes are the closest approximations to the corresponding transition states, their relative energy should reflect the outcome of the [6π]-cyclization. Indeed, it could be shown that complex **4·8** is disfavored as compared to **4·***ent*-**8**. In agreement with the experimental results, the latter complex was calculated to be more stable by 0.2 kcal/mol. From the calculation of the transition states without the host molecule **4** and the energy difference between the diastereotopic complexes, it is reasonable to assume that the host−guest interaction will influence the diastereotopic transition states. Indeed, Figure 5 nicely complements Figure 3 by showing the disfavored interaction of the cyclohexene ring with the tetrahydronaphthalene backbone in **4·8** and by demonstrating that the repulsion between the phenyl ring and the tetrahydronaphthalene is marginal in **4·***ent*-**8**.

Concluding this chapter, the enantioselective formation of intermediate *ent*-**8** in the [6π]-photocyclization reaction can be rationalized by steric interactions in the ring closure step. The preferred formation of *ent*-**8** is in line with the observed preference for the major trans enantiomer *ent*-**3a**. It is apparent, however, that the protonation of intermediates **8** and *ent*-**8** is involved in this reaction as a second selection step. A protonation must occur preferentially from the *Re*-face (relative to carbon atom C-6a) of intermediate **8** to account for the preference of *ent*-**2a** over **2a**. Deuteration experiments were undertaken to study the influence of possible proton sources more closely. Given the use of imides related to compound **4** in enantioselective protonation experiments,[22] its potential influence was to be looked at.

Deuteration Experiments. As previously discussed (schemes 1 and 4; Figure 3), the ring closure step of the

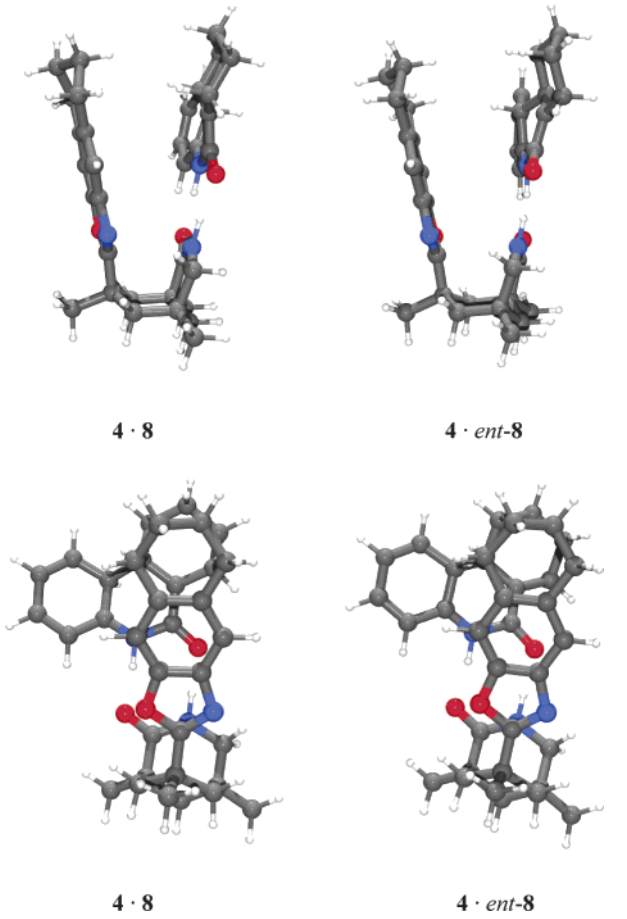

4 · **8** **4** · *ent*-**8**

4 · **8** **4** · *ent*-**8**

FIGURE 5. Diastereotopic complexes **4·8** and **4·***ent*-**8**, shown in two orientations.

[6π]-photocyclization determines the absolute configuration at carbon atom C-10a of the product. The configuration at carbon atom C-6a is established in the protonation step, which can occur intramolecularly (1,5-H shift) or intermolecularly. To distinguish between an inter- and an intramolecular protonation, the deuterated analogue d^5-**1a** of compound **1a** was prepared (Scheme 5). Acylation of cyclohexene carboxylic acid **9** with d^5-aniline gave the desired product. Its photocyclization yielded photocyclization products, the deuterium content of which was determined by ^{1}H NMR experiments. Irradiation experiments with compound d^5-**1a** were conducted at room temperature and at −55 °C in the absence and in the presence of host **4**. The most relevant results of this study are summarized in Table 3. The deuterium content in trans product **3a** (d^5-**3a** vs d^4-**3a**) remained unchanged in all runs and was roughly 65%. The deuterium content in cis product **2a** was roughly 10% in the absence of the host and 0% in its presence. The observed selectivities (trans/cis ratio, ee) did not significantly differ from the values recorded for the nondeuterated starting material (Tables 1 and 2). The trans/cis ratio was ca. 35/65 in the absence of the host at room temperature and at low temperatures (entries 1 and 3).

(22) (a) Yanagisawa, A.; Kikuchi, T.; Watanabe, T.; Yamamoto, H. *Bull. Chem. Soc. Jpn.* **1999**, *72*, 2337−2343. (b) Yanagisawa, A.; Kikuchi, T.; Kuribayashi, T.; Yamamoto, H. *Tetrahedron* **1998**, *54*, 10253−10264. (c) Potin, D.; Williams, K.; Rebek, J., Jr. *Angew. Chem., Int. Ed. Engl.* **1990**, *29*, 1420−1422.

TABLE 3. [6π]-Photocyclization of Deuterated Substrate d⁵-1a under Various Conditions with Toluene as the Solvent

entry	substrate	c_{amide} mM)	c_{host} (mM)	temp (°C)	time (min)[a]	yield (%)[b]	trans/cis[c]	ee_{trans} (%)[d]	D_{trans} (%)[e]	ee_{cis} (%)[d]	D_{cis} (%)[f]
1	d⁵-**1a**	4	0	35	120	81	33/67	0	63	0	8
2	d⁵-**1a**	4	9.6	35	120	84	49/51	39	64	33	0
3	d⁵-**1a**	4	0	−55	210	89	39/61	0	63	0	9
4	d⁵-**1a**	4	9.6	−55	210	74	62/38	64	67	26	0

[a] Time after which the conversion was complete. [b] Yield of isolated product (mixture of the two diastereoisomers). [c] Diastereomeric ratio was determined by GC analysis of the crude product mixture. [d] Enantiomeric excess was determined by chiral GC. [e] Deuterium content given in percent for racemic or enantiomerically enriched d⁵-**3a**/(d⁴-**3a** + d⁵-**3a**). The deuterium content was determined by ^{1}H NMR spectroscopy. [f] Deuterium content given in percent for racemic or enantiomerically enriched d⁵-**2a**/(d⁴-**2a** + d⁵-**2a**). The deuterium content was determined by ^{1}H NMR spectroscopy.

SCHEME 5

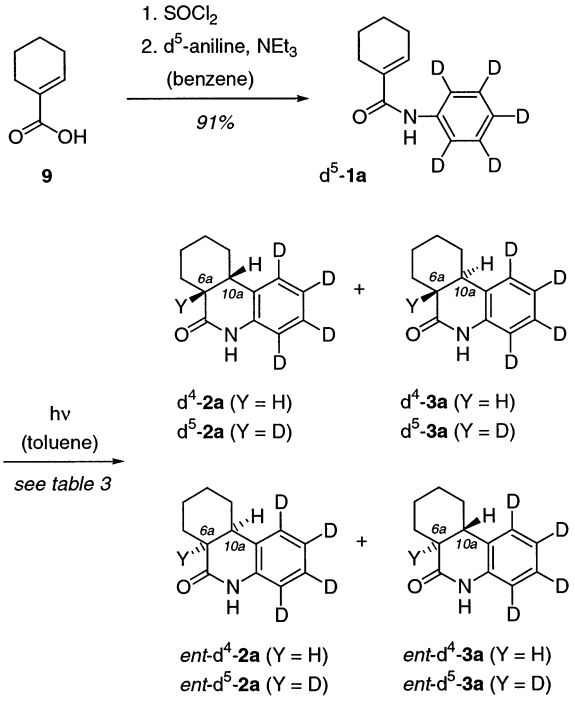

SCHEME 6

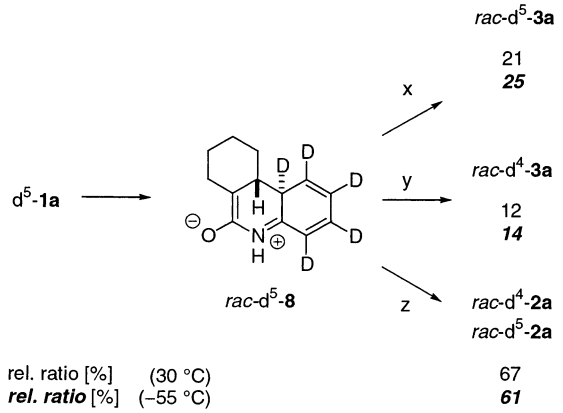

The ratio was altered in the experiments conducted in the presence of host **4** (entries 2 and 4). It was 50/50 at room temperature and 62/38 at −55 °C. Additionally, modest to good ee values were recorded in these photocyclization reactions.

What conclusions can be drawn from the deuteration data regarding the mechanism of the enamide cyclization and its control by host **4**? Pentadeuterated trans product *rac*-d⁵-**3a** is formed by an intramolecular 1,5-D-shift,[23] whereas the tetradeuterated trans and cis compounds *rac*-d⁴-**3a** and *rac*-d⁴-**2a** result from intermolecular proton-transfer processes. The small percentage (8−9%) of pentadeuterated cis compound *rac*-d⁵-**2a** produced from irradiations in the absence of host (nonhosted irradiations) was presumably formed by intermolecular deuterium transfer. In the presence of host **4**, *rac*-d⁵-**2a** was not formed at all. It was concluded that the intermolecular deuterium transfer is a minor pathway, and it was therefore neglected in the mechanistic considerations. The product distribution of nonhosted irradiations as depicted in Scheme 6 was derived from the deuterium content and the trans/cis ratio. From this, the ratios between 1,5-H-shift (*x*) and intermolecular protonation processes (*y* and *z*) were determined to be 21/79 at 30 °C and 25/75 at −55 °C. The facial diastereoselectivity of the intermolecular protonation is represented by the quotient *y*/*z*, with *y* and *z* representing the protonations to the trans and cis compounds, respectively. It was found to be 15/85 at 30 °C and 19/81 at −55 °C in favor of the formation of the cis compound.

The interplay between enantioselective ring closure and enantioselective protonation can be elucidated from the product distribution of hosted irradiations (2.4 equiv of **4**). GC analyses provided the amounts of d⁴-**2a** and *ent*-d⁴-**2a**, whereas only the total amounts of d⁴- and d⁵-**3a** and of d⁴- and d⁵-*ent*-**3a** were obtainable by this means. However, the total amount of pentadeuterated d⁵-**3a** and d⁵-*ent*-**3a** could be determined by ^{1}H NMR measurements. Estimating a single parameter in the reaction scheme allows the product distribution to be calculated from these analyses. In our view, it is reasonable to assume that the 1,5-H-shift on the face that is not shielded by the host (*x*″) occurs with the same probability as it does in the unhosted reaction, i.e., $x'' = x = 0.21$ at 30 °C and $x'' = x = 0.25$ at −55 °C. From *x*″ and the amount of d⁵-**8** calculated from total **3a** and *ent*-d⁴-**2a**, the amount of d⁵-**3a** was derived. Subsequently, the product distribution was easily obtained and is graphically depicted in Scheme 7.

As in the undeuterated case, the cyclization to the intermediate d⁵-**8**/*ent*-d⁵-**8** occurs with no enantioselectivity (2% ee) at 30 °C and moderate enantioselectivity (30% ee) at −55 °C. In intermediate *ent*-d⁵-**8**, the 1,5-D-shift is facile ($x' = 0.41$ at 30 °C and $x' = 0.51$ at −55 °C). At the same time, the host acts as a proton source and influences the protonation selectivity *y*/*z*. Enhanced

(23) For a previous study in which deuterium labeling was used to prove the intramolecular nature of the 1,5-H-shift, see: Lenz, G. R. *J. Org. Chem.* **1976**, *41*, 2201−2207.

SCHEME 7

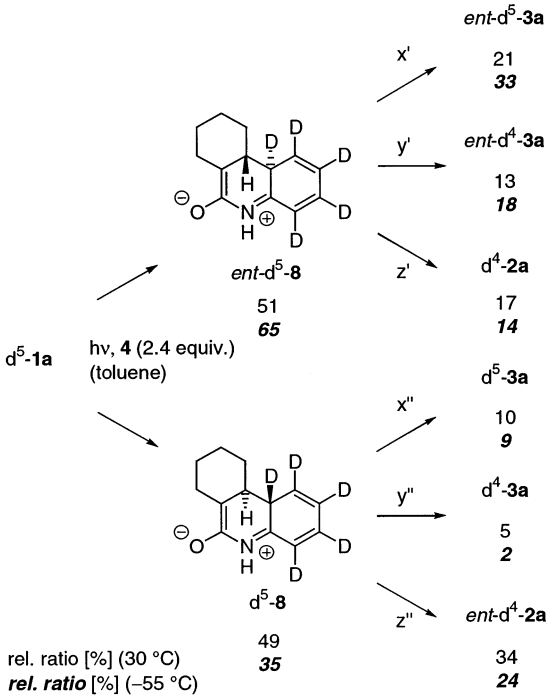

protonation of d^5-**8** from the *Re*-face (*z*″) leads to an improved selectivity of *y*″/*z*″ = 13/87 and 8/92 at 30 and −55 °C, respectively. The same effect reduces the selectivity of the protonation of *ent*-d^5-**8** to *y*′/*z*′ = 43/57 at 30 °C and even causes a reversion to 56/44 at −55 °C. This phenomenon is responsible for the astonishing variation of the observed enantiomeric excesses at different temperatures. At 30 °C, *ent*-d^4-**3a**/*ent*-d^5-**3a** (39% ee) and *ent*-d^4-**2a** (33% ee) are favored because of enhanced protonation from the shielded face (*y*′ and *z*″). At lower temperatures, the control of the protonation is accompanied by an increased control of the C−C bond-forming cyclization. In the case of the trans product, the effects complement each other because *ent*-d^4-**3a**/*ent*-d^5-**3a** are formed from the preferred intermediate *ent*-d^5-**8** upon protonation from the shielded face (*y*′) or by 1,5-D-shift (*x*′). This leads to an increased enantioselectivity of 64% ee. The opposite development holds true for the cis compound. Lactam *ent*-d^4-**2a** is formed from the disfavored intermediate d^5-**8** by the favored protonation from the shielded face (*z*″), thereby reducing its enantioselectivity to 26% ee.

If one takes into account a coordination of the intermediates **8** and *ent*- **8** to the host **4**, the protonation selectivity in favor of a *Re*-face attack is apparent. Dissociation of the guest, which is a necessary requirement for protonation by the host, opens the *Re*-face for a potential attack. While the NH···O bond is broken, the O···HN might still be intact. A potential transition state that is accessible for any intermediate **8** is schematically drawn in Figure 6. From complex **4·8** the transition state is accessed by rotation about the O···HN hydrogen bond as depicted in Figure 6. The same argument holds true for the analogous complex **4**·*ent*-**8** (Figure 3).

The increased control of the cyclization at low temperatures can be rationalized by a higher association constant of amide **1a** and host **4**. This is due to the exergonic

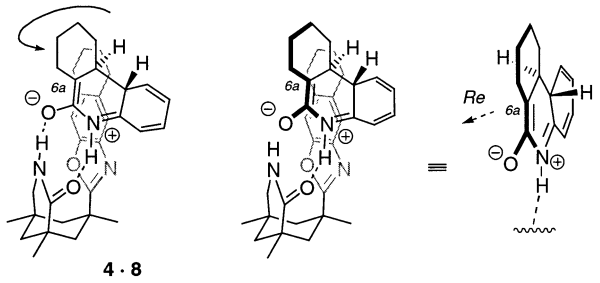

FIGURE 6. Dissociation of the NH···O bond in complex **4·8** and potential transition state for the protonation of **8** associated to host **4**.

nature of this complex formation as determined by microcalorimetry for the complex of 2-quinolone with host **4**.[16d] In addition, the stabilization of the required cis conformation of the amide in the transition state of the cyclization has a greater effect on the relative velocities of hosted and unhosted cyclizations at low temperatures. The control of the protonation step is similarly effective at 30 and −55 °C. Evidently, host **4** acts as a chiral acid with similar selectivity, regardless of whether it is involved in a defined complex by hydrogen bonds.

The fact that the mechanistic discussion is valid both for the deuterated and the undeuterated case can be concluded qualitatively from comparison of the product distributions. The D-substitution does not significantly change either the ratio of **8**/*ent*-**8**, the trans/cis ratio or the enantiomeric excesses. The protonation selectivity of the intermolecular H-transfer (*y*/*z*) must remain the same in the undeuterated case, because no D is involved. With the amount of cis product **2a** being similar, *y* and consequently the ratio of 1,5-H-shift and intermolecular H transfer (*x*/*y*) must also be comparable to the undeuterated case. Moreover, the variation of the ratio of diastereoisomers (trans/cis) in the hosted and unhosted cyclizations at different temperatures is nicely reflected by the consideration described and is in full agreement with the mechanistic picture presented above.

Conclusion

In summary, the individual steps involved in the enantioselective [6π]-photocyclization of substrate **1a** have been elucidated. Initially, the relative and absolute configuration of all possible stereoisomeric products **2a**, *ent*-**2a**, **3a**, and *ent*-**3a** was established using spectroscopic (X-ray crystallography, polarimetry, and NMR spectroscopy) and computational methods. The preferred formation of compound *ent*-**3a** in the presence of host **4** could be attributed to the preferred formation of intermediate *ent*-**8** upon conrotatory ring closure. Steric arguments that were supported by DFT calculations favor complex **4**·*ent*-**8** vs **4·8**. Finally, by irradiation of deuterated amide d^5-**1a**, the variation of the enantioselective excesses with the temperature was fully explained as a result of host **4** controlling the cyclization and acting as a chiral proton source. We are aware that the mechanistic discussion of the deuteration experiments has not included potential primary and secondary isotope effects. Although it appears as if the effects are not relevant for the stereochemical outcome, and arguments why this is the case have been given, we are

currently trying to extract additional mechanistic information from appropriate isotope labeling.

Experimental Section

General Information. All reactions involving water-sensitive chemicals were carried out in flame-dried glassware with magnetic stirring under Ar. Pyridine was distilled from calcium hydride. Common solvents [diethyl ether (Et_2O), pentane (P), methanol, ethyl acetate (EtOAc), and CH_2Cl_2] were distilled prior to use. Anhydrous NEt_3 was distilled from CaH_2. All other reagents and solvents were used as received. TLC was performed on aluminum sheets (0.2 mm silica gel 60 F_{254}) with detection by UV (254 nm) or by coloration with ceric ammonium molybdate (CAM). Flash chromatography was performed on silica gel 60 (230−400 mesh) (ca. 50 g per 1 g of material to be sparated) with the indicated eluent. ^1H and ^{13}C NMR spectra were recorded at 303 K. Chemical shifts are reported relative to tetramethylsilane as an internal reference. Apparent multiplets that occur as a result of accidental equality of coupling constants to those of magnetically nonequivalent protons are marked as virtual (virt.). The multiplicities of the ^{13}C NMR signal were determined by DEPT experiments.

Preparation of Starting Materials. The chiral host compound **4** was prepared as previously described[15] and employed in enantiomerically pure form (>95% ee), $R_f = 0.17$ (2:1 Et_2O/P). Amides **1a**[9a] and **5**[9b] were synthesized according to reported procedures. Deuterated amide d^5-**1a** was prepared analogously to the following procedure. Cyclohexene-1-carboxylic acid (600 mg, 4.76 mmol) was heated under reflux in $SOCl_2$ (5 mL) for 2.5 h. The $SOCl_2$ was removed in vacuo, and benzene (8 mL) was added. This solution was added to a solution of d_5-aniline ($C_6D_5NH_2$, 477 μL, 514 mg, 5.24 mmol) and NEt_3 (1.46 mL, 10.47 mmol) in benzene (13 mL) with ice-cooling. The resulting solution was heated under reflux for 2 h. The solution was diluted with benzene (20 mL) and washed with 1 M HCl (5 mL), water (5 mL), and brine (5 mL). The combined aqueous layers were extracted with CH_2Cl_2 (10 mL). The organic layers were dried over $NaSO_4$. After filtration, the solvents were removed in vacuo. Purification of the crude product by flash chromatography (1:1 Et_2O/P) gave a colorless solid (894 mg, 91%): $R_f = 0.58$ (1:1 Et_2O/P); mp 175−177 °C; ^1H NMR (250 MHz, $CDCl_3$) δ 1.57−1.76 (m, 4 H), 2.15−2.24 (m, 2 H), 2.30−2.37 (m, 2 H), 6.69−6.74 (m, 1 H), 7.48 (s, b, 1 H); ^{13}C NMR (62.9 MHz, $CDCl_3$) δ 21.3 (CH_2), 21.9 (CH_2), 24.2 (CH_2), 25.5 (CH_2), 113.8 ($C_{ar}D$), 133.7 (*C*═CH), 135.7 ($C_{ar}D$), 145.6 (C_{ar}), 150.2 (C═*C*H), 167.4 (CO); IR (KBr) $\tilde{\nu}$ 3270 cm^{-1} (s), 2934 (s), 2857 (w), 1659 (s), 1630 (s), 1564 (s), 1504 (vs), 1385 (s), 1328 (s), 1302 (s), 1251 (s), 922 (m), 886 (w), 828 (w), 759 (m), 695 (m); MS (70 eV, EI) *m*/*z* (%) 206 (64) [M]$^+$, 109 (100) [M − C_6D_5NH]$^+$, 81 (55) [M − C_6D_5NHCO]$^+$; HRMS (EI) calcd for $C_{13}H_{10}D_5NO$ 206.14674, found 206.14698.

General Irradiation Procedure. A solution of amide **1a**, **5**, or d^5-**1a** ($c = 4 \times 10^{-3}$ M) and of the chiral host **4** in toluene was irradiated in quartz tubes (light source for the reactions at 30 °C, Rayonet RPR 3000, $\lambda = 300$ nm; light source for the reactions at −15 and −55 °C, Original Hanau TQ 150, Vycor glass filter). The solution was not degassed, and the volume varied from 3 to 30 mL depending on the amount of amide to be reacted. After complete conversion (2−5 h), the solvent was removed in vacuo and the residue was purified by flash chromatography (irradiation products of **1a** and d^5-**1a**, 2:1 → 3:1 Et_2O/P; irradiation products of **5**, 10:1 EtOAc/MeOH). The enantiomeric excess was determined by chiral GC (2,3-di-*O*-methyl-6-*O*-TBDMS-β-cyclodextrin column). Diastereoisomers **2a**/**3a** and their deuterated derivatives were separated by reverse-phase HPLC (YMC ODS-A, 250 × 20 mm i.d., gradient = 30:70 → 60:40 CH_3CN/H_2O over 30 min), and diastereoisomers **6**/**7** could not be separated.

6a,7,8,9,10,10a-Hexahydrophenantridin-6(5*H*)-one (2a, *ent*-2a, 3a, *ent*-3a).[9a,24] Previously unreported analytical data: $R_f = 0.44$ (2:1 Et_2O/P); IR (KBr) $\tilde{\nu} = 3195$ cm^{-1} (s), 3063 (s), 2933 (s), 2846 (s), 1673 (vs), 1591 (s), 1491 (s), 1391 (s), 1295 (s), 1252 (s), 867 (s), 834 (s), 751 (s).

2a and *ent*-2a: ^1H NMR (400 MHz, $CDCl_3$) δ 1.46−1.74 (m, 8 H), 2.80 (virt. q, $^3J \cong {}^3J \cong {}^3J = 4.8$ Hz, 1 H), 2.94 (virt. dt, $^3J = 10.4$ Hz, $^3J \cong {}^3J = 4.8$ Hz, 1 H), 6.73 (d, $^3J = 7.7$ Hz, 1 H), 6.99 (virt. t, $^3J \cong {}^3J = 7.7$ Hz, 1 H), 7.13−7.17 (m, 2 H), 8.00 (s, b, 1 H); ^{13}C NMR (90.6 MHz, $CDCl_3$) δ 22.7 (CH_2), 24.5 (CH_2), 25.1 (CH_2), 29.7 (CH_2), 39.1 (CH), 40.7 (CH), 115.1 ($C_{ar}H$), 123.2 ($C_{ar}H$), 127.3 ($C_{ar}H$), 127.4 ($C_{ar}H$), 136.3 (C_{ar}), 172.6 (CO); MS (70 eV, EI) *m*/*z* (%) 201 [M$^+$] (72), 172 (22) [M − CONH]$^+$, 159 (31), 146 (100) [MH − C_4H_8]$^+$, 130 (17); HRMS (EI) calcd for $C_{13}H_{15}NO$ 201.11537, found 201.11482. ***ent*-2a:** GC (160 → 200 °C at 0.5 K/min) $t_R = 54.84$ min; $[\alpha]^{20}_D = -49.1$ (*c* 0.23, $CHCl_3$) [40% ee] (lit.[12] $[\alpha]^{20}_D = -22.9$ (*c* 0.48, $CHCl_3$)). **2a:** GC (160 → 200 °C at 0.5 K/min) $t_R = 55.47$ min.

3a and *ent*-3a: ^1H NMR (400 MHz, $CDCl_3$) δ 1.23−1.44 (m, 4 H), 1.91−1.97 (m, 2 H), 2.06 (ddd, $^3J = 14.1$ Hz, $^3J = 11.4$ Hz, $^3J = 3.7$ Hz, 1 H), 2.38−2.44 (m, 1 H), 2.46−2.51 (m, 1 H), 2.61 (ddd, $^3J = 14.1$ Hz, $^3J = 10.6$ Hz, $^3J = 3.7$ Hz, 1 H), 6.77 (d, $^3J = 7.7$ Hz, 1 H), 7.03 (vt, $^3J \cong {}^3J = 7.6$ Hz, 1 H), 7.16−7.24 (m, 2 H), 8.20 (s, b, 1 H); ^{13}C NMR (90.6 MHz, $CDCl_3$) δ 25.2 (CH_2), 25.2 (CH_2), 26.1 (CH_2), 28.7 (CH_2), 37.9 (CH), 43.2 (CH), 115.1 ($C_{ar}H$), 123.0 ($C_{ar}H$), 124.3 ($C_{ar}H$), 127.3 ($C_{ar}H$), 128.3 (C_{ar}), 136.7 (C_{ar}), 173.5 (CO); MS (70 eV, EI) *m*/*z* (%) 201 [M$^+$] (100), 172 (29) [M − CONH]$^+$, 159 (18), 146 (15) [MH − C_4H_8]$^+$, 130 (35); HRMS (EI) calcd for $C_{13}H_{15}NO$ 201.11537, found 201.11546. ***ent*-3a:** GC (160 °C → 200 °C at 0.5 K/min) $t_R = 64.34$; $[\alpha]^{20}_D = -146.1$ (*c* 0.42, $CHCl_3$) [47% ee] (lit.[12] $[\alpha]^{20}_D = -158.8$ (*c* 0.16, $CHCl_3$)). **3:** GC (160 → 200 °C at 0.5 K/min) $t_R = 63.41$ min.

6a,7,8,9,10,10a-Hexahydrobenzo[*c*][1,6]naphthyridin-6(5*H*)-one (6, *ent*-6, 7, *ent*-7).[9b] Previously unreported analytical data: $R_f = 0.30$ (96:4 EtOAc/MeOH); IR (KBr): $\tilde{\nu} = 3045$ cm^{-1} (m), 2934 (s), 2847 (m), 1682 (vs), 1584 (s), 1494 (s), 1381 (s), 1261 (s), 948 (m), 830 (s); HRMS (EI) calcd for $C_{12}H_{14}N_2O$ 202.11061, found 202.11058.

6 and *ent*-6: ^1H NMR (360 MHz, CD_3OD) δ 1.25−1.65 (m, 8 H), 2.77 (virt. q, $^3J \cong {}^3J \cong {}^3J = 4.8$ Hz, 1 H), 3.01 (virt. dt, $^3J = 10.4$ Hz, $^3J \cong {}^3J = 4.8$ Hz, 1 H), 6.76 (d, $^3J = 5.5$ Hz, 1 H), 8.12−8.16 (m, 2 H); ^{13}C NMR (90.6 MHz, CD_3OD) δ 23.8 (CH_2), 25.6 (CH_2), 26.5 (CH_2), 31.3 (CH_2), 37.7 (CH), 41.8 (CH), 111.6 ($C_{ar}H$), 146.7 (C_{ar}), 147.0 (C_{ar}), 148.8 ($C_{ar}H$), 149.5 ($C_{ar}H$), 174.9 (CO); MS (70 eV, EI) *m*/*z* (%) 202 [M$^+$] (44), 173 (35) [M − CONH]$^+$, 160 (30), 147 (100) [MH − C_4H_8]$^+$, 118 (15). ***ent*-6:** GC (190 → 215 °C at 0.5 K/min) $t_R = 77.74$ min. **6:** GC (190 → 215 °C at 0.5 K/min) $t_R = 78.55$ min.

7 and *ent*-7: ^1H NMR (360 MHz, CD_3OD) δ 1.25−1.65 (m, 4 H), 1.81−1.91 (m, 2 H), 2.06 (ddd, $^3J = 13.4$ Hz, $^3J = 11.1$ Hz, $^3J = 3.6$ Hz, 1 H), 2.24−2.27 (m, 1 H), 2.46−2.51 (m, 1 H), 2.59−2.64 (m, 1 H), 6.78 (d, $^3J = 5.5$ Hz, 1 H), 8.18−8.24 (m, 2 H); ^{13}C NMR (90.6 MHz, CD_3OD) δ 26.4 (CH_2), 26.5 (CH_2), 27.4 (CH_2), 29.6 (CH_2), 38.0 (CH), 44.5 (CH), 111.5 ($C_{ar}H$), 146.1 ($C_{ar}H$), 146.5 (C_{ar}), 147.0 (C_{ar}), 149.6 ($C_{ar}H$), 175.34 (CO); MS (70 eV, EI) *m*/*z* (%) 202 [M$^+$] (100), 173 (75) [M − CONH]$^+$, 160 (44), 147 (53) [MH − C_4H_8]$^+$, 131 (34), 118 (16). ***ent*-7:** GC (190 → 215 °C at 0.5 K/min) $t_R = 87.58$ min. **7:** GC (190 → 215 °C at 0.5 K/min) $t_R = 87.00$.

6a,7,8,9,10,10a-Hexahydro-1,2,3,4-tetradeutero-phenantridin-6(5*H*)-one (d^4-2a, *ent*-d^4-2a, d^4-3a, *ent*-d^4-3a) and 7,8,9,10,10a-Pentahydro-1,2,3,4,6a-pentadeutero-phenantridin-6(5*H*)-one (d^5-2a, *ent*-d^5-2a, d^5-3a, *ent*-d^5-3a): $R_f = 0.44$ (2:1 Et_2O/P); IR (KBr) $\tilde{\nu}$ 3181 cm^{-1} (s), 3058 (s), 2934 (s), 1674 (vs), 1567 (s), 1387 (s), 1286 (m), 840 (m), 656 (m), 626 (m), 598 (m); HRMS (EI) calcd for $C_{13}H_{11}D_4NO$ 205.14047, found 205.14049; calcd for $C_{13}H_{10}D_5NO$ 206.14674, found 206.14679.

d^4-2a and *ent*-d^4-2a (92%) and d^5-2a and *ent*-d^5-2a (8%): ^1H NMR (400 MHz, $CDCl_3$) δ 1.36−1.84 (m, 8 H), 2.80 (virt. q, $^3J \cong {}^3J \cong {}^3J = 4.4$ Hz, 0.92 H), 2.95 (virt. dt, $^3J = 10.2$ Hz, $^3J \cong {}^3J = 5.1$ Hz, 1 H), 8.00 (s, b, 1 H); ^{13}C NMR (90.6 MHz, $CDCl_3$) δ 22.7 (CH_2), 24.4 (CH_2), 25.1 (CH_2), 29.7 (CH_2), 39.0

(CH), 40.7 (CH), 114.7 (t, ^1J (C, D) = 23.9 Hz, $C_{ar}D$), 122.7 (t, ^1J (C, D) = 24.1 Hz, $C_{ar}D$), 126.9 (t, ^1J (C, D) = 24.7 Hz, $C_{ar}D$), 126.9 (t, ^1J (C, D) = 25.4 Hz, $C_{ar}D$), 128.4 (C_{ar}), 136.2 (C_{ar}), 172.7 (CO); MS (70 eV, EI) *m/z* (%): 206 [d^5-M^+] (14), 205 [d^4-M^+] (59), 177 (5) [d^5-M − CONH]$^+$, 176 (20) [d^4-M − CONH]$^+$, 163 (30), 151 (24) [d^5-MH − C_4H_8]$^+$, 150 (100) [d^4-MH − C_4H_8]$^+$, 134 (17). ***ent*-d⁴/d⁵-2a:** GC (160 → 200 °C at 0.5 K/min) t_R = 53.36 min. **d⁴/d⁵-2a:** GC (160 → 200 °C at 0.5 K/min) t_R = 53.79 min.

d⁴-3a and *ent*-d⁴-3a (33%) and d⁵-3a and *ent*-d⁵-3a (67%): ^{1}H NMR (500 MHz, $CDCl_3$) δ 1.27−1.45 (m, 4H), 1.94−1.99 (m, 2H), 2.10 (ddd, ^3J = 14.0 Hz, ^3J = 11.5 Hz, ^3J = 4.3 Hz, 0.33 H), 2.41−2.46 (m, 1 H), 2.51−2.54 (m, 1 H), 2.62−2.68 (m, 1 H), 7.87 (s, b, 1 H); ^{13}C NMR (90.6 MHz, $CDCl_3$) δ 25.2 (CH_2), 26.1 (CH_2), 26.2 (CH_2), 28.8 (CH_2), 37.8 (COCD*C*H), 37.9 (COCH*C*H), 42.9 (t, ^1J (C, D) = 18.7 Hz, CO*C*DCH), 43.3 (CO*C*HCH), 114.6 (t, ^1J (C, D) = 23.8 Hz, $C_{ar}D$), 122.5 (t, ^1J (C, D) = 25.1 Hz, $C_{ar}D$), 124.0 (t, ^1J (C, D) = 24.4 Hz, $C_{ar}D$), 126.9 (t, ^1J (C, D) = 24.4 Hz, $C_{ar}D$), 128.4 (C_{ar}), 136.6 (C_{ar}), 173.2 (CO); MS (70 eV, EI) *m/z* (%) 206 [d^5-M^+] (100), 205 [d^4-M^+] (48), 177 (23) [d^5-M − CONH]$^+$, 176 (21) [d^4-M − CONH]$^+$, 163 (22), 151 (18) [d^5-MH − C_4H_8]$^+$, 150 (18) [d^4-MH − C_4H_8]$^+$, 135 (49). ***ent*-d⁴/d⁵-3a:** GC (160 → 200 °C at 0.5 K/min) t_R = 62.49. **d⁴/d⁵-3a:** GC (160 → 200 °C at 0.5 K/min) t_R = 61.59 min.

***N*-Methyllactam *ent*-2b by N-Methylation of Lactam *ent*-2a.** To a solution of lactam *ent*-**2a** (4.1 mg, 0.02 mmol, 40% ee) in dry DMF (1 mL) was added KO*t*Bu (4.5 mg, 0.04 mmol). After the mixture was stirred for 15 min at room temperature, a solution of MeI (2.5 μL, 5.7 mg, 0.04 mmol) in dry DMF (0.5 mL) was added. Following overnight stirring, the mixture was diluted with 1 N HCl (10 mL). Extraction with CH_2Cl_2 (2 × 10 mL) followed by washing of the organic extracts with water (2 × 10 mL) and brine (10 mL), drying with Na_2SO_4, and removal of the solvent in vacuo gave a light yellow oil. The crude product was purified by HPLC (YMC ODS-A, 250 × 20 mm i.d.; gradient = 50:50 → 80:20 CH_3CN/H_2O over 30 min, t_R = 16.49 min) to give a colorless oil (2.3 mg, 53%): R_f = 0.72 (1:1 Et_2O/P); ^{1}H NMR (500 MHz, $CDCl_3$) δ 1.21−1.65 (m, 8 H), 2.77 (m, 1 H), 2.89 (m, 1 H), 3.37 (s, 3 H), 6.96 (d, ^3J = 8.2 Hz, 1 H), 7.03 (vt, $^3J \cong {}^3J$ = 7.4 Hz, 1 H), 7.16 (d, ^3J = 7.4 Hz, 1 H), 7.23−7.26 (m, 1 H). ***ent*-2b:** GC (125 → 180 °C at 0.5 K/min) t_R = 71.64 min; $[\alpha]^{20}_D$ = −48.5 (*c* 0.11, in $CHCl_3$) [40% ee] (lit.[12] $[\alpha]^{20}_D$ = −53.9 (*c* 0.36, $CHCl_3$)). **2b:** GC (125 → 180 °C at 0.5 K/min) t_R = 72.45 min. All other spectroscopic data were in accordance with reported data.[9a]

***N*-Methyllactam *ent*-3b by N-Methylation of Lactam *ent*-3a.** Lactam *ent*-**3a** (5.2 mg, 0.025 mmol, 47% ee) was converted into the *N*-methyl compound by the aforementioned procedure. Chiral GC-analysis of the crude product showed a 9:1 mixture of trans compound *ent*-**3b** (47% ee) and cis isomer **2b** (46% ee). Compound *ent*-**3b** was purified by HPLC (YMC ODS-A, 250 × 20 mm i.d.; gradient = 50:50 → 80:20 CH_3CN/H_2O in 30 min, t_R = 17.96 min) to give a colorless oil (4.0 mg, 72%): R_f = 0.75 (1:1 Et_2O/P); ^{1}H NMR (360 MHz, $CDCl_3$) δ 1.21−1.41 (m, 4 H), 1.88−1.92 (m, 2 H), 2.00 (ddd, ^3J = 15.0 Hz, ^3J = 11.6 Hz, ^3J = 3.8 Hz, 1 H), 2.37−2.45 (m, 2 H), 2.55 (ddd, ^3J = 14.1 Hz, ^3J = 10.7 Hz, ^3J = 3.8 Hz, 1 H), 3.36 (s, 3 H), 6.98 (d, ^3J = 7.3 Hz, 1 H), 7.03 (t, $^3J = {}^3J$ = 7.5 Hz, 1 H), 7.23−7.27 (m, 2 H). ***ent*-3b:** GC (125 → 180 at 0.5 K/min) t_R = 88.34 min; $[\alpha]^{20}_D$ = −193.9 (*c* 0.16, $CHCl_3$) [47% ee] (lit.[12] $[\alpha]^{20}_D$ = −158.8 (*c* 0.16, $CHCl_3$)). **3b:** GC (125 → 180 °C at 0.5 K/min) t_R = 88.83 min. All other spectroscopic data were in accordance with reported data.[9a]

X-ray Crystallography. General Remarks. Crystals suitable for diffraction experiments were selected in perfluorinated ether. Preliminary examination and data collection were carried out at the window of a rotating anode X-ray generator and graphite monochromated Mo Kα radiation (λ = 0.71073 Å), controlled by the COLLECT software package.[25] Collected images were processed using Denzo. Decay effects were corrected during the scaling procedure.[26] The structures were solved by direct methods[27,28] and refined with standard difference Fourier techniques.[29] All non-hydrogen atoms of the asymmetric unit were refined with anisotropic thermal displacement parameters. All hydrogen atoms were found in the difference Fourier maps and refined freely with individual isotropic thermal displacement parameters, except those located at the disordered atoms, which were placed in calculated positions (riding model). Full-matrix least-squares refinements were carried out by minimizing $\Sigma w(F_o^2 - F_c^2)^2$ with the SHELXL-97 weighting scheme and stopped at maximum shift/err < 0.001. Crystallographic data (excluding structure factors) for the structures reported in this paper have been deposited with the Cambridge Crystallographic Data Centre as supplementary publication nos. CCDC-191141 (**1a**), CCDC-191139 (**2a**), and CCDC-191140 (**3a**). Copies of the data can be obtained free of charge upon application to CCDC, 12 Union Road, Cambridge CB2 1EZ, UK (fax, (+44)1223-336-033; e-mail, deposit@ccdc.cam.ac.uk).

Compound 3a. $C_{13}H_{15}NO$, M_r = 201.26 g/mol, colorless fragment, size 0.25 × 0.33 × 0.69 mm, triclinic, space group $P\bar{1}$ (No. 2), a = 6.3016(3) Å, b = 8.7289(4) Å, c = 10.1131(5) Å, α = 104.554(2)°, β = 105.514(2)°, γ = 96.646(3)°, V = 508.73(4) Å^3, Z = 2, ρ_{calcd} = 1.314 g/cm^3, μ(Mo Kα) = 0.083 mm^{-1}, F(000) = 216, T = 173 K. The cyclohexane part of the molecule is disordered over two positions (90.5:9.5). Hydrogen atoms of the major part were found and refined freely. The final model (213) parameters were refined to wR_2 = 0.1167 based on all 1873 data, R_1 = 0.0425 based on 1600 data with $I \geq 2\sigma(I)$, GOF = 1.064, and min/max residual electron density = −0.18/0.18 e/Å^3.

Computational Details. The density functional/Hartree−Fock hybrid model Becke3LYP[20] implemented in GAUSSIAN-98[21] has been used throughout this study together with the 6-31G(d) basis set. All geometries have been fully optimized. Frequency calculations for **1a**, **4**, *ent*-$\mathbf{8_{TS}}$, **8**, and *ent*-**8** ensured that they either correspond to minima (NIMAG 0) or transition states (NIMAG 1) on the potential energy surface. Complete details can be found in Supporting Information.

Acknowledgment. We thank Prof. Stefan Grimme (Universität Münster) for calculating the specific rotation of compounds **2a** and **3a**. This work was supported by the Fonds der Chemischen Industrie and by the Deutsche Forschungsgemeinschaft. B.G. is grateful to the Fonds der Chemischen Industrie for a Kekulé fellowship.

Supporting Information Available: Cartesian coordinates of all calculated structures and crystal data, details of the structure in the solid state together with PLATON[30] graphics, and X-ray crystallographic files for compounds **1a**, **2a**, and **3a**. This material is available free of charge via the Internet at http://pubs.acs.org.

JO026602D

(24) Masamune, T.; Takasugi, M.; Suginome, H.; Yokohama, M. *J. Org. Chem.* **1964**, *29*, 681−685.
(25) Hooft, R.; Nonius, B. V. *COLLECT, Data Collection Software for Nonius KappaCCD Devices;* Nonius: Delft, The Netherlands, 1998.
(26) Otwinowski, Z.; Minor, W. In *Processing of X-ray Diffraction Data Collected in Oscillation Mode*; Carter, C. W., Jr., Sweet, R. M., Eds.; Academic Press: New York, 1997; Vol. 276, pp 307−326.
(27) Altomare, A.; Cascarano, G.; Giacovazzo, C.; Guagliardi, A.; Burla, M. C.; Polidori, G.; Camalli, M. *J. Appl. Crystallogr.* **1994**, *27*, 435−441.
(28) Sheldrick, G. M. *SHELXS-86*; Universität Göttingen: Göttingen, Germany, 1997.
(29) Sheldrick, G. M. *SHELXL-97*; Universität Göttingen: Göttingen, Germany, 1998.
(30) Spek, A. L. *PLATON, A Multipurpose Crystallographic Tool*; Utrecht University: Utrecht, The Netherlands, 2001.